

## Repetitive, triggered, long life-time spark-gap switch for pulsed power applications

G.J.J. Winands, Z. Liu, A.J.M. Pemen, E.J.M. van Heesch and K. Yan

*EPS Group, Department of Electrical Engineering, Eindhoven University of Technology,  
5600 MB, Eindhoven, The Netherlands, e-mail: [g.j.j.winands@tue.nl](mailto:g.j.j.winands@tue.nl)*

Non-thermal plasmas for gas cleaning purposes can be generated in various ways. In this paper, a critical component for pulsed plasma generation is described: a spark-gap switch. The design of a coaxial, high repetition rate, large average power, and long-life time switch is discussed. The switch is used with a fail-free LCR trigger circuit. Critical issues for switch design are presented with experimental results. It is observed that the switch has a good stability, and its lifetime is estimated to be in the order of  $4 \cdot 10^{10}$  shots.

### Introduction

One promising way to generate non-thermal plasma is by using a pulsed power source [1-3]. The most critical component in these kinds of sources is the heavy-duty closing switch. For large scale industrial corona applications using ultra-short nano-pulses, magnetic compression switches or spark gap switches are usually used. Main disadvantage of the magnetic compression switch is its lower energy efficiency for ultra-short pulses ( $\sim 50$ ns). For spark-gap switches, the lifetime was the mayor limiting factor. Other difficulties with spark-gaps are related to: pulse repetition rate, electrode material erosion, insulator degradation, arc-inductance, hold-off voltage, and triggering.

In this paper, a newly developed coaxial spark-gap switch having large, brass, electrode surfaces is described. Because of the design of the electrodes, a lifetime up to  $4 \cdot 10^{10}$  shots can be guaranteed. The spark gap is pressurized (up to 7 bars, to increase hold-off voltage and to decrease inductance and resistance) and continuously flushed with air (up to  $35 \text{ Nm}^3/\text{hr}$ , for increased pulse repetition rate, to remove spark-residue from the gap, and to cool down the electrodes). The switch is used with an LCR trigger circuit, for reliable switching behavior. When operated in a correct regime, the LCR circuit always causes the switch to close at the right moment [3].

### Construction of the spark-gap switch

In Figure 1, a schematic overview of the designed coaxial spark gap is shown. Because of the short (2 mm, Table 1) electrode-trigger distance, the inductance of the switch is small. The coaxial structure ensures an impedance of  $25\Omega$  during switching, which is matched to both a pulse forming line and a two stage transmission line transformer.

Several mechanism are responsible for the long (estimated) life-time of the switch ( $\sim 4 \cdot 10^{10}$  shots, 10 J/pulse). Firstly, a large volume of electrode

material is allowed to be evaporated before the gap distance becomes too large for proper switching. Especially the trigger-electrode surface is large. Even when a layer of the electrode material is evaporated, the switch can still be used; simply by decreasing the pressure [3]. Secondly, brass is used as electrode material, which is known for its low evaporation rate. Lastly, due to the switch design, the “moving arc” principle applies. Due to magnetic pinching, any arc initiated between the electrodes will start moving towards the centre of the switch. The arc is thus not confined to one spot, but moves along the surface. As a result the problem caused by the hot-spots becomes less sever.

The use of a forced gas-flow ensures the possibility to use high pulse repetition rate (kpps). Because of the direction of the flow (arrows in Figure 1), the spark residue and eroded electrode material cannot reach the insulator surfaces. This way, surface flash-over on the high-voltage feed-through are prevented. Possible damage to the insulator surface due to radiation of the spark is limited due to the small opening angle of the radiation coming from the electrode-trigger gap.

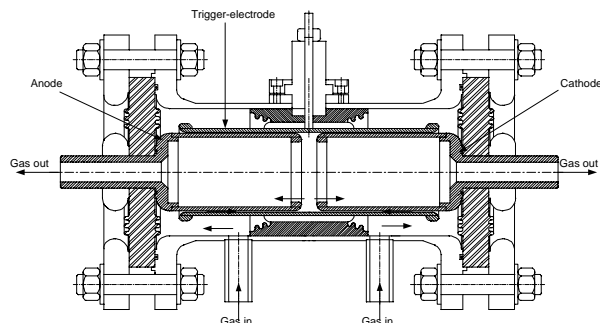


Figure 1: Construction drawing of the coaxial spark-gap switch. The arrows in the bottom part indicate the direction of the forced gas flow.

Table 1: Characteristics of the coaxial spark-gap switch.

Anode/Cathode	Material	Brass	Anode-Trigger distance	2 mm
	Length	114 mm	Max. pressure	7 bar
	Diameter	61 mm	Max. flow rate	35 Nm <sup>3</sup> /hr
Trigger electrode	Material	Brass	Impedance	25 Ω
	Length	202 mm	Repetition rate	< 1 kpps
	Diameter	65 mm	Switching voltage	~ 60 kV
Ground structure	Material	Stainless Steel	Average power	~ 10 kW
	Length	252 mm		
	Diameter	108 mm		

### LCR trigger-circuit

Figure 2 shows the connection of the LCR circuit and the switch to the power source.

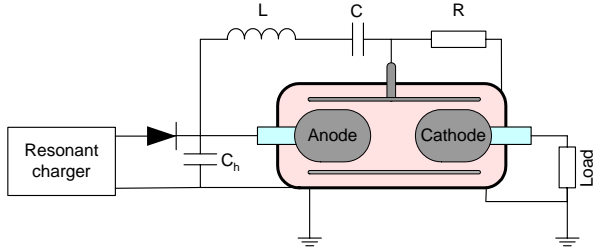


Figure 2: Switch and trigger connections.

To illustrate the mechanism of the LCR circuit, the following equations are useful. Reference [3] can be used to obtain the complete circuit of the source. The charging voltage  $V$  on the anode is:

$$V(t) = \frac{V_{\max}}{2} \cdot (1 - \cos(\omega_2 \cdot t)). \quad (1)$$

Where  $V_{\max}$  is the maximum voltage on  $C_h$  and  $\omega_2$  is the resonant charging frequency of the source. During the charging of  $C_h$ , the voltage  $V_T$  on the trigger electrode changes as:

$$V_T(t) = \frac{V_{\max}}{2} \cdot \frac{\omega_2^2 \cdot \tau_{LCR}^2}{1 + \omega_2^2 \cdot \tau_{LCR}^2} \cdot \left( \exp\left(-\frac{t}{\tau_{LCR}}\right) - \cos(\omega_2 \cdot t) \right) + \frac{V_{\max}}{2} \cdot \frac{\omega_2 \cdot \tau_{LCR}}{1 + \omega_2^2 \cdot \tau_{LCR}^2} \cdot \sin(\omega_2 \cdot t) \quad (2)$$

Where  $\tau_{LCR} = R \cdot C$  is the time-constant of the trigger circuit. The value of  $\tau_{LCR}$  determines the voltage ration  $V_T(t)/V(t)$  after charging of  $C_h$  ( $t = \pi/\omega_2$ ). In Figure 3, the voltage potentials on anode and trigger electrode are plotted as function of time.

Since resonant charging is used as basic mechanism for energy storage in the high-voltage capacitor, the voltage on the switch will rise as a sine-function. The voltage on the trigger-electrode also rises as a sine-function, only with lower amplitude and some time-delay. Once the charging process is finished, the voltage on the anode remains constant (as long as  $C_h \gg C$ ), but the voltage on the trigger-electrode will decrease, with time constant  $\tau_{LCR}$ . As a result the voltage difference between anode and trigger increases

exponentially, leading in the end to an arc-plasma ( $\approx 30$  MHz, oscillation in the LC circuit) across the anode-trigger gap. Now, the voltage difference between trigger and cathode rises drastically, leading to complete closure of the switch. This trigger method is independent on electrode geometry and charging voltage. If the switch is operated in a correct V-p regime, the switch will always fire, due to the ever increasing voltage difference between the anode and trigger electrode.

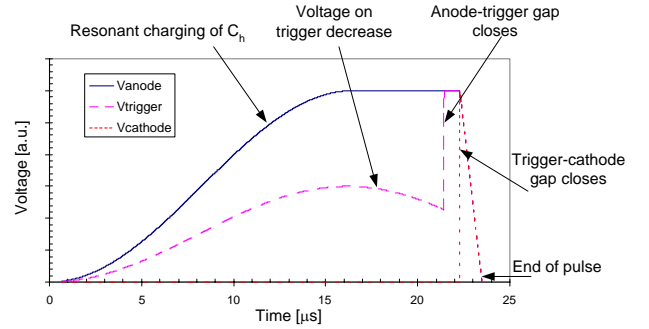


Figure 3: Schematic representation of the voltage on the anode, cathode and trigger electrode. For clarity, the pulse length ( $V_{\text{cathode}}$ ) is drawn about 10 times longer than the one mentioned in Table 1.

Because of the geometry of the coaxial spark-gap switch, it is important that during charging, the voltage difference between anode and trigger, and that between cathode and trigger remains equal. Otherwise the switch could pre-fire. Due to the switch design, this means that the maximum voltage on the trigger-electrode should be 50% of the anode voltage. The voltage on the trigger electrode can be adjusted by changing the components of the LCR circuit.

### Experimental results and Discussion

The pressure drop over the switch and the flow connections (about 20 meter long tubing) was determined to be around 0.2 bars. To validate the system design, several measurements were performed. The generated pulses on the load contain about 1 J per pulse, with a pulse duration of

100 ns (FWHM), and a peak-current of 300 A. To be able to measure at high pulse repetition rates a wire-plate reactor was used as a load. All voltage measurements were performed using a differentiating-integrating measuring system [4]. Measurements concerning the voltage, pressure, pulse repetition rate, and flow rate are shown in Figure 4 and 5. For all measurements, the average (1000 shots) switching voltage was around 34 kV.

Up to 450 pulses per second (pps) no flush gas flow was needed to prevent pre-firing, only the pressure inside the gap had to be increased (Figure 4b). Apparently, the increased pressure improves the recovery time of the switch. For most spark-gap switches, the pressure cannot be changed significantly, because the operational V-p range is small. However, the typical design of the coaxial spark-gap switch, together with the LCR trigger method, enables operation over a broad pressure range.

In general it can be stated that the obtained recovery time of  $\sim 2$  ms, for an un-flushed switch, is very short compared to the work reported earlier by other authors [9-11]. The exact reason for this short recovery time is not completely understood yet, but it is believed that it is due to the combination of short gap-distance and large electrode surfaces. The electrodes act as heat-sink, quickly restoring the gas-temperature to the initial temperature. Ions generated during the spark move to the electrodes in a short period, because of the short distance.

The solid markers shown in Figure 4b indicate the critical situation for stable triggering (34 kV). Below the markers, the switch is in the pre-fire mode. Far above the markers, very late-firing or miss-firing may occur.

Besides stabilizing the switch by means of increasing the pressure, the spark-gap can also be stabilized by increasing the gas-flow rate. Instead of using the output air-flow rate as measure, it was chosen to look at the effects of the absolute air-velocity inside the spark-gap. In Figure 5, the velocity-pressure as function of pulse repetition rate dependency is shown. For conditions below the markers, the switch is pre-firing. Far above the markers, the switch may miss-fire. The results clearly demonstrate the beneficial use of both pressure and flow as stabilization method.

Another interesting topic for switches is the switching time-delay and its jitter. Because the break-down process is statistical in nature, the time between complete charging of the anode and closing of the switch varies (time delay). When monitoring a large number of shots, the time delay

distribution will become “bell” shaped. The width of this shape, measured at half the maximum value (FWHM), is used as a measure for the time jitter.

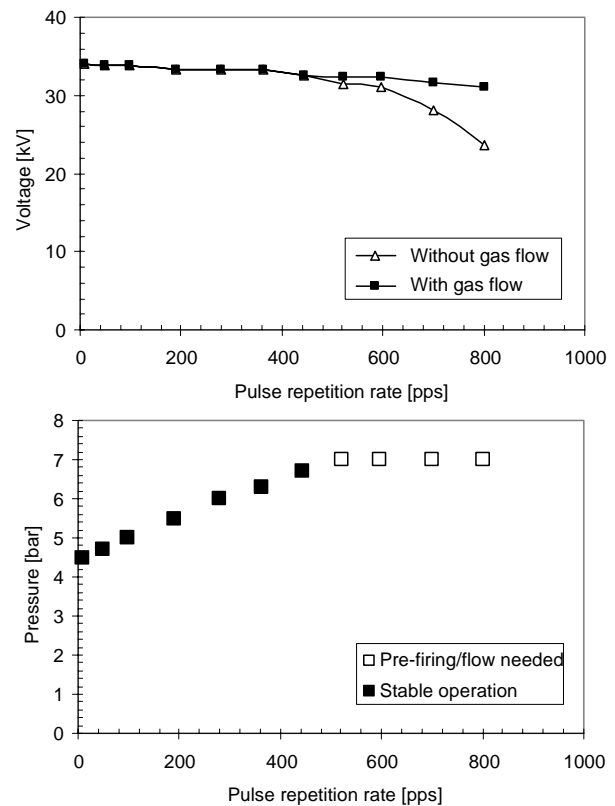


Figure 4: a) Average switching voltage as function of pulse repetition rate. For higher frequencies the pressure was increased, so no flow was required. The small decrease that can be observed for the “with gas flow” line is due to the used resonant charger. b) Pressure-pulse repetition rate dependence for stable switch performance. Above 450 pps, also flow was needed.

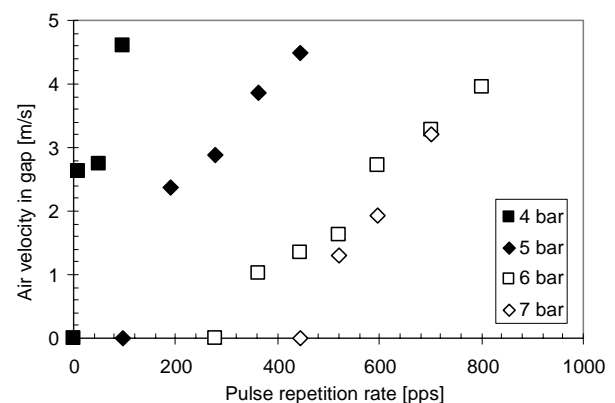


Figure 5: Required air-velocity and pressure, for stable switching performance, as function of pulse repetition rate. The maximum pulse repetition rate (820 pps) was limited by the resonant charging unit.

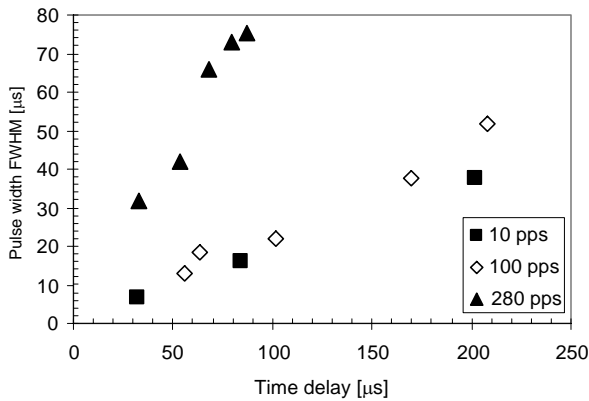


Figure 6: Jitter as function of time-delay and pulse repetition rate. All markers are the result of averaging over 1000 pulses.

For the measurements shown in Figure 6, the maximum pulse repetition rate was limited to 280 pps. All markers are the result of averaging over 1000 pulses.

Clearly, for higher repetition rates, the time-delay and jitter have similar values. Late-firing and miss-firing cannot be observed anymore, only firing directly or shortly after the charging is observed.

Measurements regarding the lifetime have not been finished yet, since this can only be done after a large amount of switching has been done (mass difference measurement). However, to indicate the uniform erosion of the electrode surface, a photograph of the anode is shown in Figure 7. At the time of the picture about  $10^6$  shots were performed (Energy 1~5 J/pulse).

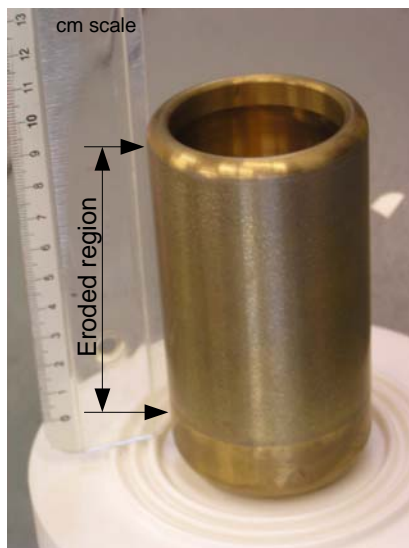


Figure 7: Photograph of one of the electrodes. The photograph was taken after about  $10^6$  shots (Energy 1~5 J/pulse). The white disc at the bottom is the Teflon high-voltage feed through, with a special profile to increase the surface flashover voltage (see Figure 1).

## Conclusion

A newly designed coaxial spark-gap switch for pulsed power applications has been described. Due to the large electrode surfaces, the choice of electrode material, and the “moving arc” principle, the estimated lifetime of the switch is  $4 \cdot 10^{10}$  shots (with  $\sim 10$  J/pulse). An LCR trigger-circuit is used for stable operation of the switch. Air pressure and flow rate in the switch can be controlled separately, so that the switch can be used for different voltages and pulse repetition rates in a good switching regime. The presented results show that by increasing the pressure, pre-firing can be prevented up to 450 pps (average switching voltage 34 kV), without the use of a forced air-flow. The ability to use a wide pressure range is an advantage resulting from the switch design. Forced air-flow can also be used for preventing pre-firing. The switch was operated up to 820 pps, with 7 bars of pressure and airflow rate of  $32 \text{ Nm}^3/\text{hr}$ . It is preferable to use the smallest possible pressure, in combination with the required flow rate, because the flow removes the evaporated electrode material from the switch. Also, for a fixed gap-distance, the spark inductance decreases for lower pressures.

The flow rate and pressure of the gap also have an influence on the time-delay between charging and closing of the gap. Also the jitter of the time-delay can be influenced. Miss-firing and very late-firing can be prevented by using just sufficient pressure and air-flow.

Several measurements that will be performed, and reported on, in the near future are:

- Life-time test, erosion rate estimation,
- Switching stability test for long operation,
- Performance at different switching voltages,
- Performance with matched/unmatched loads.

## References

- [1] G.J.J. Winands, K. Yan, S.A. Nair, A.J.M. Pemen, E.J.M. van Heesch, *Plasma Processes and Polymers*, Vol. 2, No. 3, 2005, pp. 232-237.
- [2] K. Yan, G.J.J. Winands, S.A. Nair, E.J.M. van Heesch, A.J.M. Pemen, I. de Jong, *J. Adv. Oxid. Technol.*, **7** (2004) 116-122.
- [3] K. Yan, “Corona Plasma Generation”, Ph.D. thesis, Eindhoven University of Technology, (2001).
- [4] M.A. van Houten, “Electromagnetic Compatibility in High-Voltage Engineering”, Ph.D. thesis, Eindhoven University of Technology, (1990).